PROGRESSIVE FATIGUE DAMAGE MODELLING OF CFRP LAMINATES AT THE MESOSCALE LEVEL

K.I. Tserpes
Laboratory of Technology & Strength of Materials
Dept of Mechanical Engineering & Aeronautics
University of Patras, Patras GR-26500, Greece

P. Papanikos
ISTRAM, Institute of Structures & Advanced Materials
Patron-Athinon 57 St., Patras GR-26441, Greece

Th. Kermanidis
Laboratory of Technology & Strength of Materials
Dept of Mechanical Engineering & Aeronautics
University of Patras, Patras GR-26500, Greece

Abstract

A mesomechanics based progressive fatigue damage model for assessing fatigue damage initiation, propagation and life of Carbon- Fibre-Reinforced Plastics (CFRP) laminates is presented. A meso-volume concept is proposed such as to incorporate the main microscopic failure mechanisms and allow the usage of continuum mechanics as a tool for predicting these failure mechanisms. The size of the meso-volume is determined by the condition of satisfactory accuracy in an affordable computational time. The model comprises the components of stress analysis using finite elements, fatigue failure analysis and fatigue material property degradation. In the specific application, the meso-volume corresponds to the 3-D element of the laminate FE model. Predicted results in the form of fatigue life prediction and edge delamination initiation and propagation are compared with respective experimental data obtaining a good correlation. The introduced model is understood as the background for the development of a fatigue damage tolerance concept for composite ageing aircraft components.

Keywords: meso-volume, composite laminates, fatigue, progressive damage modelling, delamination

1. Introduction

Generally, the term mesomechanics is used to describe the intermediate level of material description between micromechanics (dislocations and unit voids and inclusions) and macromechanics (specimen). This classification cannot be taken as exhaustive. For instance, Panin [1] suggested even a more detailed classification with meso-I and meso-II levels. Many of the researchers defined the meso-level as a range of scale levels determined in terms of material size. For example, Mishnaevsky and Schmauder [2] following Needleman's [3] definition for 'mesoscale continuum mechanics' defined meso-level as a range of scale levels, which are 2-3 orders of magnitude greater than the defects of the structure (which are varied at the $10^{-9}...10^{-5}$ m scale range) and 1-3 orders of magnitude smaller than a specimen or workpiece.

To the author's opinion, the definition of meso-level using fixed scale ranges is justified from the physical viewpoint but may decrease the effectiveness of mesomechanics based concepts to deal with engineering problems appreciably. In engineering applications acceptable solutions are expected to comprise satisfactory accuracy in an affordable computational time. Hence, the thorough selection of the scale levels is essential. Based on the above, in what follows, the selection of the material meso-level scale range will be understood as flexible and application specific. It is believed that from the engineering viewpoint it suffices to define the meso-level scale range such as to comprise two main features: (a) the involvement of the main micro-mechanisms controlling the materials mechanical behaviour and failure and (b) the applicability of the continuum mechanics equations. Within the above defined scale range the material meso-volumes may be chosen such as to minimize the computational effort for the required accuracy. In the present paper, the above viewpoint will be exploited to investigate the problem of fatigue in composite laminates.

Although aeronautical industry is the primary user of composites, fatigue of composite aircraft components has not been encountered yet according to its real impact on the engineering aircraft design. This can be explained by the fact that the stress levels, which develop during service are low and far from the design limits, and by the belief that composites are not prone to fatigue. However, in the last few years the problem of fatigue in composite aircraft components has gained importance emanating from the facts: (a) that many aircrafts incorporating composite parts are now ageing aircrafts and therefore, sensitive to wide-spread fatigue damage (especially delamination) [4,5] and (b) that the stress levels that exist around stress concentrators of the aircraft fuselage such as composite bolted joints are high and not too far from design limits.

A very important issue in the assessment of advanced composites behavior is the choice of analysis scale. In the macroscopic scale the analyses are empirical and case specific. On the other hand, in the microscopic scale the analyses may become overwhelming when including the complex failure mechanisms, which are due to high anisotropy and inhomogeneity of the composite material. Hence, it is essential to develop concepts closing the gap between the micro- and macro-scale analysis levels.

In this paper, a Fatigue Progressive Damage Model (FPDM) is developed on the basis of such a concept, the meso-volume concept. The FPDM is able to assess fatigue damage initiation, propagation and life of CFRP laminates. It comprises the components of stress analysis (FE modelling), fatigue failure analysis and fatigue material property degradation. In the specific application, the meso-volume corresponds to the 3-D element of the laminate FE model. The case study of Fibredux-HTA/6376 laminates subjected to tension-compression (T-C) fatigue is considered to illustrate the model capabilities. The paper closes with a short discussion of the progress of development at the Laboratory of Technology and Strength of Materials of a Fatigue Damage Tolerant Design (FDTD) concept for composite ageing aircraft components.

2. The meso-volume concept

The meso-volume is defined in each problem according to the requirements of involvement of the micro- failure mechanisms and the applicability of equations of continuum mechanics to predict the initiation and propagation of these failure mechanisms. The meso-volume concept can be used in both homogeneous and inhomogeneous material problems.

In the problem of fatigued CFRP laminates, the meso-volume corresponds to the 3-D layered element of the laminate FE model, which was developed using the ANSYS FE code [6]. Fig.1 shows a schematic drawing of the meso-volume (ANSYS 3-D 8-noded SOLID46 layered element [6]) used to model the laminate. It is defined by layer direction and thickness and orthotropic material properties. In each meso-volume one layer was modelled in order to achieve better accuracy in the interlaminar normal and shear stresses.

The components of the FPDM (stress analysis, failure analysis and fatigue material property degradation) are applied in meso-volume basis in an iterative procedure. First, continuum mechanics (laminate plate theory) are used to calculate the 3-D stresses field in each meso-volume and then using stress-based failure criteria seven different microscopic failure modes are predicted. The material properties of each meso-volume are degraded in two ways. Gradual degradation driven by the number of cycles is implied in all meso-volumes while sudden degradation in the meso-volumes where failure has been detected. The components along with this procedure will be explained in detail in the following sections.

The size of the meso-volume is decided with regard to the laminate dimensions such as to achieve good accuracy in the calculated stresses. Special attention was given in the mesh density at the free edges where the edge effect leads to high interlaminar normal and shear stresses and therefore, to early delamination initiation. However, the mesh density is restricted by the total number of meso-volumes, which determines the computational time and computer storage. Fig.3 shows the mesh of the laminate used in this work.

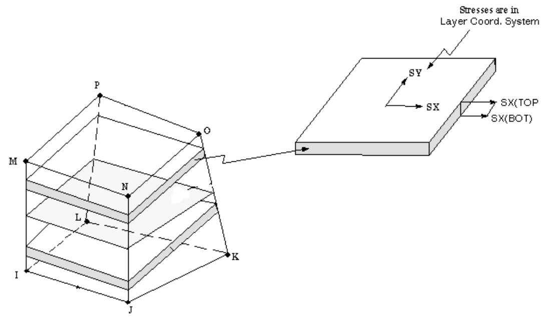

Figure 1: *A schematic illustration of the meso-volume, after [6]*

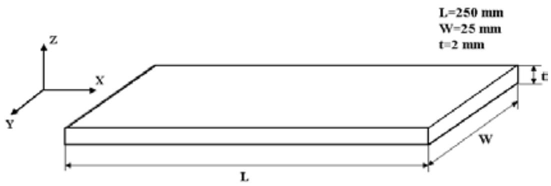

Figure 2: *A schematic drawing of the laminate*

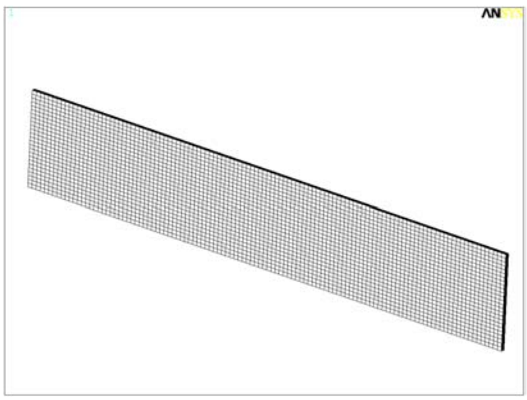

Figure 3: *FE mesh of the laminate*

3. Fatigue failure analysis

Seven polynomial fatigue failure criteria were used to detect seven failure modes. Specifically, for detecting matrix tensile and compressive cracking, fibre compressive failure and fibre-matrix shear-out, a set of 3-D Hashin-type fatigue failure criteria [7] were used while for detecting fibre tensile failure delamination in tension and compression the Maximum Stress and the Ye-delamination [8] criteria were used, respectively. These failure modes represent the main microscopic failure mechanisms that may exist in the composite meso-volume. The fatigue failure criteria with regard to failure modes are as follows.

Matrix tensile cracking, for $(\sigma_{yy} > 0)$:

$$\left(\frac{\sigma_{yy}}{Y_T^F}\right)^2 + \left(\frac{\sigma_{xy}}{S_{xy}^F}\right)^2 + \left(\frac{\sigma_{yz}}{S_{yz}^F}\right)^2 \geq 1 \qquad (1)$$

Matrix compressive cracking, for $(\sigma_{yy} < 0)$:

$$\left(\frac{\sigma_{yy}}{Y_C^F}\right)^2 + \left(\frac{\sigma_{xy}}{S_{xy}^F}\right)^2 + \left(\frac{\sigma_{yz}}{S_{yz}^F}\right)^2 \geq 1 \qquad (2)$$

Fibre tensile failure, for $(\sigma_{xx} > 0)$:

$$\left(\frac{\sigma_{xx}}{X_T^F}\right) \geq 1 \qquad (3)$$

Fibre compressive failure, for $(\sigma_{xx} < 0)$:

$$\left(\frac{\sigma_{xx}}{X_C^F}\right) \geq 1 \qquad (4)$$

Fibre-matrix shear-out, for $(\sigma_{xx} < 0)$:

$$\left(\frac{\sigma_{xx}}{X_C^F}\right)^2 + \left(\frac{\sigma_{xy}}{S_{xy}^F}\right)^2 + \left(\frac{\sigma_{xz}}{S_{xz}^F}\right)^2 \geq 1 \qquad (5)$$

Delamination in tension, for $(\sigma_{zz} > 0)$:

$$\left(\frac{\sigma_{zz}}{Z_T^F}\right)^2 + \left(\frac{\sigma_{xz}}{S_{xz}^F}\right)^2 + \left(\frac{\sigma_{yz}}{S_{yz}^F}\right)^2 \geq 1 \qquad (6)$$

Delamination in compression, for $(\sigma_{zz} < 0)$:

$$\left(\frac{\sigma_{zz}}{Z_C^F}\right)^2 + \left(\frac{\sigma_{xz}}{S_{xz}^F}\right)^2 + \left(\frac{\sigma_{yz}}{S_{yz}^F}\right)^2 \geq 1 \qquad (7)$$

In the above equations, σ_{ij} are the layer stress components in the *ij* directions. They refer to a local layer coordinate system, in which the *x* and *y*-axes are parallel and transverse to the fibres, respectively, while the *z*-axis coincides to the normal direction. In the denominators appear the corresponding strengths, in which the superscript *F* refers to fatigue strengths and the subscripts *T, C* refer to the tensile and compressive value of the strengths, respectively.

When composite structures are subjected to fatigue loading, the material is loaded by a stress state, which is at the first cycles of loading less than the strength of the material. Therefore, at the first cycles there is no static mode of failure. By increasing the number of cycles, the stiffness and strength of the material degrade due to the nature of cyclic loading. The degradation of stiffness leads to stress redistributions and thus, to higher stress states, which in combination with degraded strength values lead to static failures. To consider this feature, the degraded strengths were used in the above failure criteria instead of the static strengths. This is the only difference between the static and fatigue failure criteria.

4. Fatigue material property degradation

In static loading cases, material degradation is applied when a sudden mode of failure is detected by the failure criteria. This type of degradation is called *sudden material property degradation* and is applied by using an appropriate sudden degradation rule, which disables the failed material region from carrying a specific load. In fatigue loading cases, the nature of cycling loading implies an additional material degradation, which is independent of detection of sudden failure and is driven by the increased number of cycles. This type of degradation is called *gradual* *material property degradation*. Both types of degradation are implemented in this work in meso-volume basis and will be discussed in the following Sections.

Sudden degradation

When failure is predicted in a meso-volume by the failure criteria of Eqs (1)-(7), its elastic properties and strengths are degraded by implementing an appropriate *sudden degradation rule*. To date, sudden degradation rules have been applied only in static progressive damage models. In Ref [9], the authors have reported work on this topic by examining the effect of sudden material property degradation rules on predicted load-displacement curves and failure loads of bolted composite joints. As a result of this investigation, a new set of sudden degradation rules, which imposed a realistic degradation of the material, and lead to very good agreement between the predicted and experimental failure loads was proposed. This set was also used in the present FPDM and is depicted in Table 1. (The superscript *d* refers to the degraded value of the material property).

Mode of failure	Sudden degradation rule
Matrix tensile cracking	$E^d_{yy}=0.2*E_{yy}$, $G^d_{xy}=0.2*G_{xy}$, $G^d_{yz}=0.2*G_{yz}$
Matrix compressive cracking	$E^d_{yy}=0.4*E_{yy}$, $G^d_{xy}=0.4*G_{xy}$, $G^d_{yz}=0.4*G_{yz}$
Fibre tensile failure	$E^d_{xx}=0.07*E_{xx}$
Fibre compressive failure	$E^d_{xx}=0.14*E_{xx}$
Fibre-matrix shear-out	$G^d_{xy}=v_{xy}=0$
Delamination in tension and compression	$E^d_{zz}=G^d_{yz}=G^d_{xz}=v_{yz}=v_{xz}=0$

Table 1: *Sudden material property degradation rules*

Gradual degradation

The gradual degradation of the composite material due to the cyclic loading, was applied on the basis of meso-volume stiffness and strength. The gradual degradation modelling is described in the following two Sections.

The residual stiffness of composite laminates subjected to fatigue loading has been studied by many researchers with both theoretical and experimental methods. The residual stiffness has been also used as fatigue damage parameter in order to predict life of the laminates. A large number of the studies were concerned with quasi-isotropic CFRP laminates due to their importance in aeronautical applications. These studies have indicated a similar fatigue-induced stiffness degradation for all quasi-isotropic CFRP laminates, which was influenced slightly by the maximum applied stress of the fatigue loading. In particular, stiffness showed an almost linear degradation with respect to number of cycles.

Fig.4 show the normalized residual stiffness of the $[45/0/-45/90_2/-45/0/45]_S$ quasi-isotropic Fiberdux-HTA/6376 laminate subjected to T-C fatigue for different stress levels obtained experimentally in [10]. From this figure it is clear that the stiffness degraded in the manner described above. As may be seen, there is a small influence of the maximum applied stress in the final value of the normalized residual stiffness just before failure.

In the current work, to model the gradual degradation of stiffness of the laminates as a function of number of cycles, linear equations derived from fitting of the data in Fig.4 for each stress level, were used. The general form of the linear equations in terms of normalized residual stiffness and normalized number of cycles is

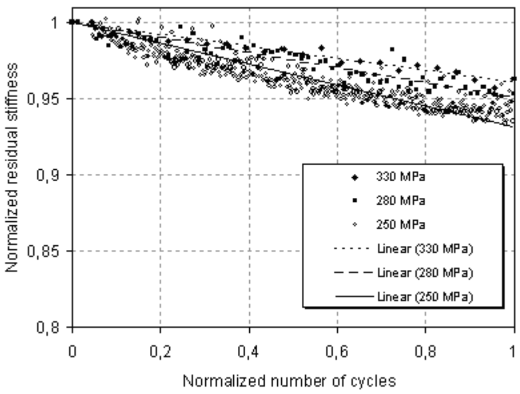

Figure 4: *Normalized residual stiffness of the Fiberdux-HTA/6376 laminate subjected to T-C fatigue under different stress levels, after [10].*

$$E(n) = [A(n/N_f) + 1]E_S \quad (8)$$

where E and E_S are the residual and the static stiffnesses, respectively, n the number of cycles, N_f the number of cycles to failure, and A an experimental fitting parameter. It is assumed that this degradation applies to all directions of the laminate.

In the same way to stiffness, the gradual degradation of strength was modelled by fitting the experimental data. Fig. 5 shows the experimental normalized residual tensile strength of the Fibredux-HTA/6376 subjected to T-C fatigue loading together with fitting curves for three different stress levels [10].

For the fitting of the normalized residual strength as function of the number of cycles, second order polynomials were chosen. The general form of the polynomials in terms of normalized residual strength and normalized number of cycles is

$$T(n) = [B(n/N_f)^2 + C(n/N_f) + 1]T_S \quad (9)$$

where T and T_S are the residual and static strengths, respectively, n the number of cycles, N_f the number of cycles to failure, and B, C experimental fitting parameters.

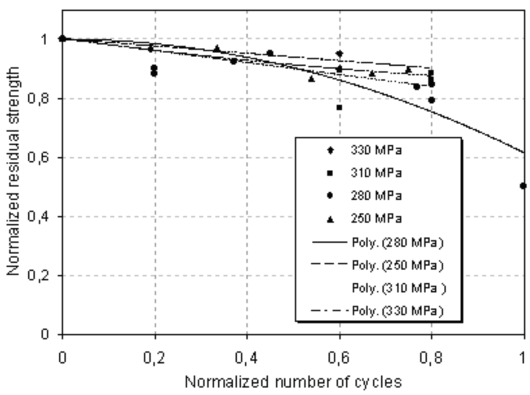

Figure 5: *Normalized residual strength of the Fiberdux-HTA/6376 laminate subjected to T-C fatigue under different stress levels, after [10]*

The choice of the polynomials was done because the normalized residual strength degraded in a bigger range than residual stiffness and ended in a smaller value of the static strength at the number of cycles to failure. Eq.(9) is used to model the degradation of all strength components.

5. Modelling of cyclic loading

In contrast to static loading, the numerical modelling of cyclic loading is a very difficult task. More specific, if it is desired to model the load cycle by cycle the function describing the cycle must be followed exactly. This would demand to choose as many points as possible on the entire function and apply to the FE model the loads that correspond to the selected points. As it can be understood, this is impossible to be performed from the point of view of CPU time and computer storage even for a single cycle and not for the thousands of cycles that are usually applied to real problems.

On the other side, it is important to consider the effect of the *R* ratio in each problem. For example, in the case of reversed cyclic loading (*R*=-*1*), both the tensile and compressive loads have a significant effect on the developed damage mechanisms and therefore, on the number of cycles to failure.

In the present model, a new methodology has been used in order to apply the cyclic loading in the FE model. This methodology is based on the following assumptions:

(a) in each cycle, only the maximum and minimum loads are applied based on the assumption that damage initiates only at these loads,

(b) for the number of cycles equal to the chosen increment only gradual degradation of the material and not sudden is considered.

To illustrate the methodology, consider the case of T-C loading (*R*=-*1*) and the prediction of fibre tensile (fibre breakaway) and fibre compressive (fibre buckling) failure modes through Eqs (3) and (4), respectively. In each cycle, only the $\sigma_{\max}$ tensile load is applied in the laminate, the induced stresses are calculated by the FE model and a check for possible failure modes is performed. For example, the induced tensile $\sigma_x > 0$ stresses are checked with Eq.(3) for possible fibre tensile failure. Then, based on the elastic solution of the laminate, in order to find the stresses that would induced by the application of the compressive $\sigma_{\min} = R\sigma_{\max} = -\sigma_{\max}$ loading, the previous calculated stresses are multiplied by the *R* ratio giving in the specific example $R\sigma_x = -\sigma_x < 0$. Finally, the check for possible fibre compressive failure using Eq.(4) is performed. This procedure incorporates the above mentioned assumptions, is repeated for all stress components and for all failure modes, and can be followed for any stress ratio *R*.

6. Flowchart of the FPDM

The previously described components of the FPDM have been programmed in the ANSYS FE code in order to create a user-friendly macro-routine, which is described by means of the flowchart shown in Fig.6.

1. Development of the 3-D FE model of the composite laminate. Definition of geometry, stacking sequence, initial (static) material properties and loading conditions (maximum applied stress, stress ratio and increment of number of cycles).
2. Performing linear stress analysis to calculate and store the 3-D stress field in each meso-volume. The stresses are calculated with respect to a local layer coordinate system as shown in Fig.3.
3. Performing fatigue failure analysis by applying the failure criteria of Eqs (1)-(7).
4. Check for ply failures in the meso-volumes.
   - 4.1 If no failure is predicted, increase the number of applied cycles *n* by *Δn*, perform gradual degradation of stiffness and strength of the meso-volumes using Eqs (8) and (9) and return to step 2.
   - 4.2 If any mode of failure is detected continue to the next step.
5. Performing sudden degradation of material properties of the meso-volumes by applying the rules of Table 1.
6. Check for catastrophic failure of the laminate.
   - 6.1 Stop, if final failure is reached.
   - 6.2 If not, return to step 2 and perform again linear stress analysis to calculate the redistributed stresses.

This procedure is repeated until final failure occurs.

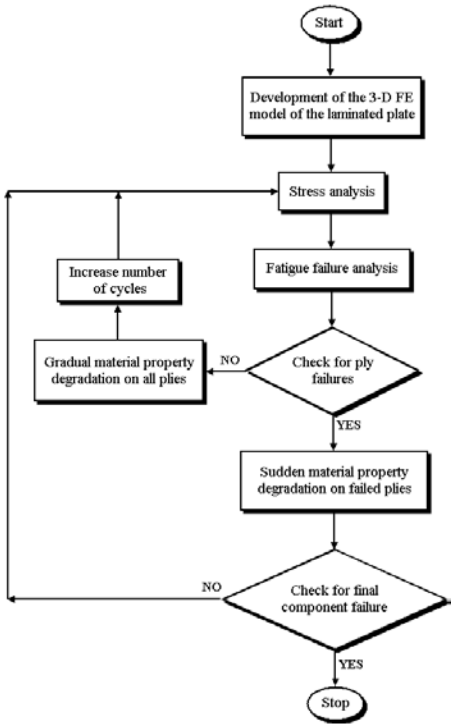

Figure 6: *Flowchart of the FPDM*

7. Fatigue life prediction

The FPDM was applied to the thermosetting Fiberdux-HTA/6376 laminates subjected to T-C loading ($R=\sigma_{min}/\sigma_{max}=-1$), and the results were compared with the experiments of [10]. The stacking sequences of the laminates was $[45/0/-45/90_2/-45/0/45]_S$. The static material properties of the Fiberdux-HTA/6376 lamina are shown in Table 2.

Material property	Fiberdux-HTA/6376
E_{xx}	137 GPa
$E_{yy}=E_{zz}$	9.9 GPa
$G_{xy}=G_{xz}$	5.2 GPa
G_{yz}	3.1 GPa
$\nu_{xy},\ \nu_{xz},\ \nu_{yz}$	0.3
X_T	2090 MPa
$Y_T=Z_T$	75 MPa
$Y_C=Z_C$	168 MPa
$S_{xy}=S_{xz}$	42 MPa
S_{yz}	26 MPa

Table 2. *Static material properties of the Fiberdux-HTA/6376 lamina*

The dimensions of all specimens were 250mm x 25mm x 2mm, as showed in Fig.2. The length of the specimens modelled was reduced in both sides by the length of the tabs (50mm) used in the experiments. The results in form of life prediction and damage accumulation are presented in the following Sections.

Fig.7 shows the comparison between the predicted and experimental [10] *S-N* curves for the $[45/0/-45/90_2/-45/0/45]_S$ Fiberdux-HTA/6376 laminate subjected to T-C fatigue. The dotted lines in the graph of the figure are best fits of the experimental data while the solid lines are best fits of the predicted data. The selected stress levels ranged from 240 to 365 MPa. For each stress level, the linear and polynomial functions resulted from fitting of the corresponding experimental data were used for modelling the gradual degradation of stiffness and strength, respectively. The procedure described in section 2 for the stress levels appeared in Figs 4 and 5 was followed for all the stress levels in the *S-N* curves.

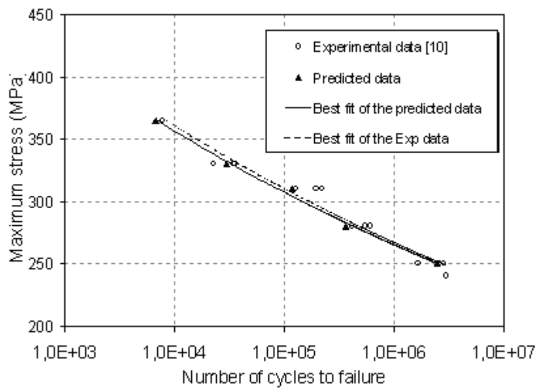

Figure 7: *Predicted and experimental S-N curves of the Fibredux-HTA/6376 laminates subjected to T-C fatigue*

As may be seen from Fig.7, a very good agreement, which is within the experimental scatter, has been achieved. To give an example, at the load of 330 MPa the mean experimental N_f was 31126 cycles while the predicted was 32400 cycles (Δn=600 cycles). Therefore, it can be stated that the

FPDM predicts the fatigue life successfully.

8. Edge delamination propagation

Fig.8 shows the prediction of delamination growth for different fractions of laminate life compared with the respective C-scan graphs of the fatigued specimens for the stress level of 280 MPa. It is clear, that the model describes satisfactory the trend of edge delamination evolution. Delamination initiated in both cases at an early stage of loading at the laminate free edges and propagated normal to the loading direction towards the middle of the specimen with the increased number of cycles.

In Fig.8 it is also shown the C-scan of the reference specimen, which indicates the presence of appreciable initial damage at the free edges along the longitudinal direction as well as at some internal areas. A detail observation of sequence of the C-scan graphs shows clearly that delamination initiated not only from the laminate free edges but also from the internal initial damage areas. A big percent of the damage accumulated in the center of the specimen initiated from these areas. In the prediction of Fig.8, the initial damage was not considered in the FPDM.

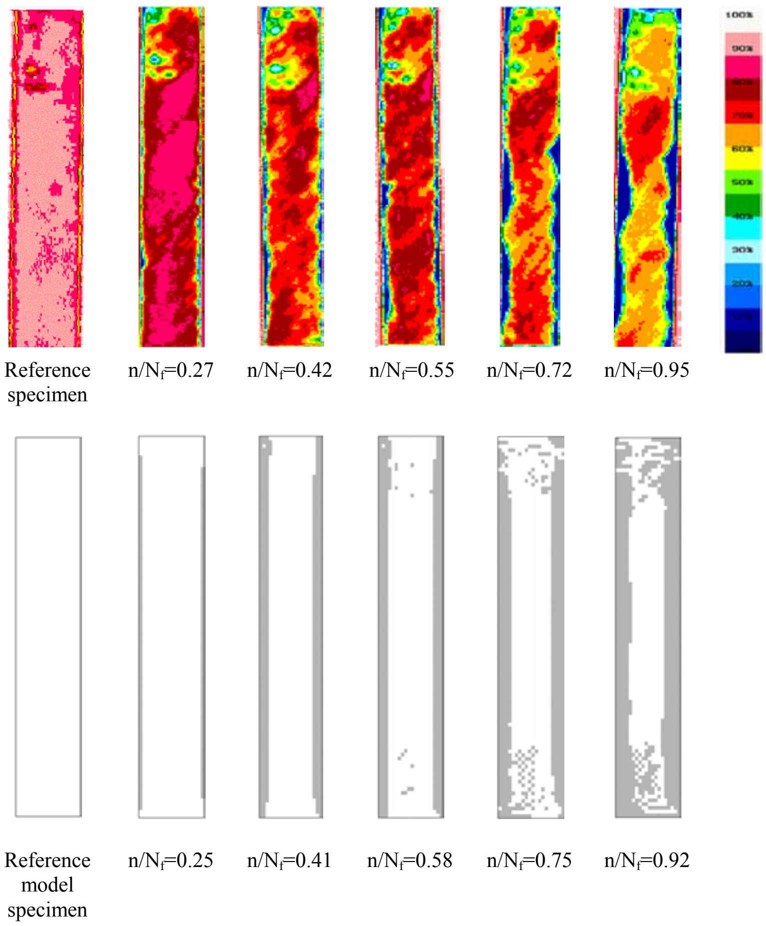

Figure 8: *Predicted and experimental edge delamination propagation*

This is the reason for not predicting accurately the delamination in the internal areas of the specimen. By performing a detail study of the effect of initial damage on delamination onset and growth it was found that at the edges it is not necessary to consider initial damage because the high interlaminar stresses lead to prediction of delamination onset at a very early stage of the cyclic loading. On the other hand, the consideration in the FPDM of the internal initial damage was proved significant.

9. Towards a fatigue damage tolerance design

In Ref [4], the issue of ageing in composite aircraft components has been discussed and the basis of the development of a mesomechanics based FDTD concept to deal this issue was set. This concept is a combination of the FPDM with a meso-damage parameter (DSF). The DSF was formulated in [10,11] to quantify the qualitative information obtained from C-scan graphs of fatigued specimens similar to those appear in the first part of Fig.8. Therefore, the DSF is actually a quantification of the macroscopic representation of the microscopic failure mechanisms evolution and is defined at the mesoscale level at the same scale with the meso-volume presented in this work.

References

[1]. Panin, V.E. (ed) (1998), *Physical Mesomechanics of Heterogeneous Media and Computer-Aided Design of Materials.* Cambridge Internat Sci Publishing, 1998.

[2]. Mishnaevsky, L.M. and Schmauder S. (2001), ‘‘Continuum mesomechanical finite element modeling in materials development: A state-of-the-art review’’, *Appl Mech Rev*, **5(1)**, pp. 156-178.

[3]. Needleman, A. (2000) ‘‘Computational mechanics at the mesoscale’’, *Acta Mater*, **48(1)**, pp. 105-124.

[4]. Pantelakis, Sp., Tserpes, K.I. (2002), ‘‘Fatigue damage modelling and life assessment of ageing composite aircraft components’’, Proceedings of the GRACM2002 Congress on Computational Mechanics, Patras, June 27-29.

[5]. Papanikos, P., Tserpes, K.I. and Pantelakis, Sp. (2002), ‘‘Modelling of fatigue damage progression and life in CFRP laminates’’, *submitted for publication.*

[6]. ANSYS User’s Manual. (2001) Version 5.6. Swanson Analysis Systems, Inc.

[7]. Hashin, Z. (1980) ‘‘Failure criteria for unidirectional fibre composites’’. *Journal of Applied Mechanics*. **47,** 329-334.

[8]. Ye, L. (1988) ‘‘Role of matrix resin in delamination onset and growth in composite laminates’’. *Comp Sci Tech*, **33**, pp. 257-277.

[9]. Tserpes, K.I., Labeas, G., Papanikos, P. and Kermanidis, Th. (2001) ‘‘Strength prediction of bolted joints in graphite/epoxy composite laminates’’. *Comp Part B: Engng,* in press.

[10]. Pantelakis, Sp.G., Kyriakakis, Em.Ch. and Papanikos, P. (2001), ‘‘Non-destructive fatigue damage characterization of laminated thermosetting fibrous composites’’. *Fatigue Fract Engng Mater Struct*, **24(10)**, pp. 651-662.

[11]. Pantelakis, Sp.G. and Kyriakakis, Em.Ch. (1999), ‘‘Fatigue damage of APC-2 composite assessed from material degradation and non-destructive evaluation data’’, *Theor Appl Fract Mech,* **32**, pp. 37-46.